

## Idiotypic–Anti-Idiotypic Complexes and Their In Vivo Metabolism

Amanda Johansson, M.D., Ph.D.<sup>1</sup>

Ann Erlandsson, B.S.<sup>2</sup>

David Eriksson, B.S.<sup>1</sup>

Anders Ullén, M.D., Ph.D.<sup>1</sup>

Patrik Holm, B.S.<sup>2</sup>

Birgitta E. Sundström, Ph.D.<sup>2</sup>

Kenneth H. Roux, Ph.D.<sup>3</sup>

Torgny Stigbrand, M.D., Ph.D.<sup>1</sup>

<sup>1</sup> Department of Immunology, Umeå University, Umeå, Sweden.

<sup>2</sup> Division for Chemistry, Karlstad University, Karlstad, Sweden.

<sup>3</sup> Department of Biological Science, Structural Biology Program, Florida State University, Tallahassee Florida.

Presented in poster form at the Eighth Conference of Radioimmunodetection and Radioimmunotherapy of Cancer, Princeton, New Jersey, October 12–14, 2000.

Supported by grant no. 1387 from the Swedish Cancer Research Council; the Lions Foundation in Umeå, Sweden; the University of Umeå, Sweden; and the National Institutes of Health grant no. R21 AI 144291 (awarded to K.H.R.).

Address for reprints: Amanda Johansson, M.D., Ph.D., Department of Immunology, Umeå University, S-901 87 Umeå, Sweden; Fax: +46 90 7852250; E-mail: amanda.johansson@climi.umu.se

Received October 31, 2001; accepted November 14, 2001.

**BACKGROUND.** Different strategies can be used to improve the tumor:non-tumor ratio of radiolabeled antibodies in immunotargeting. One approach is to use secondary antibodies to clear out redundant, circulating primary antibodies. In the current study, the in vitro complex formation and in vivo clearing capabilities and metabolism of the monoclonal antibody TS1 and its monoclonal anti-idiotypic,  $\alpha$ TS1, were studied.

**METHODS.** Complex formation studies were performed using polyacrylamide gel electrophoresis (PAGE), gel permeation chromatography, and electron microscopy. The clearance and metabolism of the complexes were studied in nude mice.

**RESULTS.** PAGE and gel permeation chromatography showed that more than 70% of the antibodies formed complexes. The electron microscopy studies revealed that the complexes formed between TS1 and  $\alpha$ TS1 are mainly ring-shaped (66.6–73.4%), comprising 4 to > 8 antibodies. These rings consist of equal numbers of idiotype and anti-idiotypic. The most commonly observed complexes were tetrameric rings (26.8–40.5%), hexameric rings (10.7–11.9%), and rings containing more than eight monoclonal antibodies (6.6–14.4%). The in vivo study illustrated that within 24 hours 80% of the total nuclide content had been degraded and excreted via the urine, compared with 25% for similarly treated mice that did not receive any anti-idiotypic.

**CONCLUSIONS.** Interestingly, the electron microscopy study demonstrated that dimers were rare (0.4–1.2%), probably reflecting a location of epitopes incompatible with tight, sterically constrained dimeric interactions; insufficient flexibility of the immunoglobulin G1 subtype hinge regions; or both. The anti-idiotypic clearing mechanisms proved efficient in nude mice. In vivo metabolic studies indicate that the accumulation and degradation of TS1/ $\alpha$ TS1 immune complexes, to a large extent, take place in the liver, where a substantial amount was detected as soon as 1 hour after anti-idiotypic injection. *Cancer* 2002;94:1306–13.

© 2002 American Cancer Society.

DOI 10.1002/cncr.10301

**KEYWORDS:** anti-idiotypic, idiotype, immune complex, metabolism, TS1.

**R**adioimmunotherapy (RIT) and radioimmunolocalization (RIL) are developing and promising techniques for diagnosing and treating tumors by use of radiolabeled antibodies (Ab) targeting tumor-specific antigens.<sup>1–3</sup> The therapeutic index, i.e., the relationship between the antitumor effect and normal tissue toxicity, determines the utility of an anticancer therapy.<sup>1</sup> For RIT in particular, the radiolabeled Abs exert toxic side effects. A variety of strategies have been shown to alter the therapeutic index of radiolabeled Abs, by either increasing the accumulation of nuclide in the tumor or decreasing the amount of radiation delivered to normal tissues. Optimization of the tumor:nontumor ratio (T/N) remains an ongoing process within the field. Several approaches have been, and currently are being, studied

in order to accomplish satisfactory clearing of nontargeted idiotypic (Id) Abs. One approach is to utilize smaller Ab fragments, i.e., Fab, F(ab')<sub>2</sub> or ScFv, which clear the circulation of the host more rapidly than intact Abs, due to their smaller size and lack of Fc domain. However, this rapid clearance has resulted in less total tumor uptake compared with intact molecules, making them more useful for imaging than therapy.<sup>4–6</sup> Other techniques to improve the T/N include two- or multistep procedures, based on the high-affinity avidin-biotin interaction, or reduction of the circulating nontargeted Ab in vivo by extracorporeal immunoadsorption, where the hosts' blood is cleared of circulating Ab using an on-line Ab adsorption column.<sup>7</sup> Another possibility is to use secondary, anti-idiotypic (anti-Id) Abs, which rapidly and with high specificity clear the circulation from the Id Ab, potentiating an increase in T/N of up to 10-fold.<sup>8–11</sup> The immune complexes formed between the Id and anti-Id are efficiently taken up by the reticuloendothelial system and degraded, followed by excretion of radioiodinated species in the urine.<sup>11</sup>

The monoclonal Ab (MAb) TS1, which targets a recently defined epitope on cytokeratin (CK) 8,<sup>12</sup> has proved efficient in several experimental radioimmunotargeting studies.<sup>13,14</sup> By use of the syngeneic anti-Id  $\alpha$ TS1, directed against TS1, the total body radioactivity in nude mice bearing subcutaneous HeLa-cell tumors could be decreased by 80–85%, resulting in a two- to threefold increase in T/N within 24 hours of anti-Id injection.<sup>9</sup> The affinity constant ( $K_A$ ) between TS1 and  $\alpha$ TS1 has been determined to be  $8.6 \times 10^{10}$  using biosensor technology (BIAcore 2000, Uppsala, Sweden).<sup>11</sup>

The use of syngeneic anti-Id MAbs offers several advantages. First, the method requires no complicated, surgical intervention; second, there is no risk of leakage of contaminants from the immunoadsorption columns (e.g., anti-Abs, avidin, or streptavidin), thus avoiding potential secondary immunizations; third, the immune system of the host remains intact, since only the administered MAb and its antiidiotypic are eliminated; and, finally, the removal of Id is rapid and the amount to be removed is controllable.<sup>9</sup>

The aims of the current study were to evaluate the immunochemical interaction patterns in vitro between TS1 and its anti-Id,  $\alpha$ TS1, and to investigate the clearing capabilities of the anti-Id and the metabolic fate of immune complexes formed between TS1 and  $\alpha$ TS1 in vivo.

## MATERIALS AND METHODS

### Monoclonal Antibodies

The anti-CK MAb TS1 (immunoglobulin [Ig]G $\kappa$ ) and its anti-Id,  $\alpha$ TS1 (IgG1 $\kappa$ ), were obtained from InRo Biomedtek (Umeå, Sweden).<sup>9,15</sup>

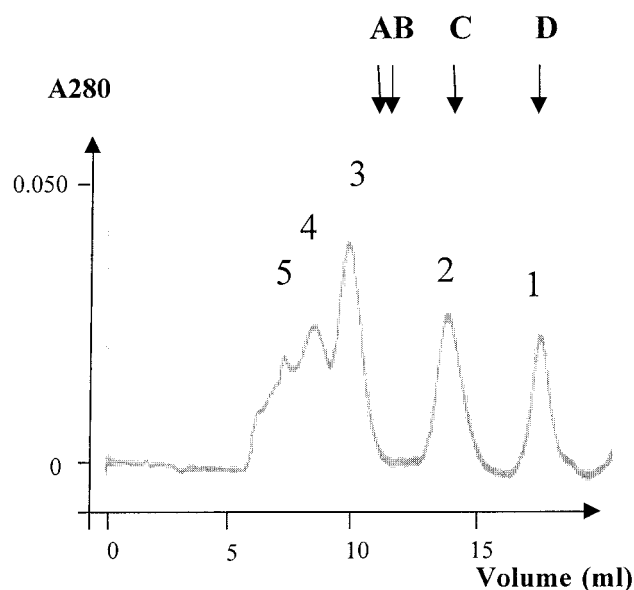


**FIGURE 1.** Chromatogram of TS1- $\alpha$ TS1 in a 1:1 ratio on Superose 6. Arrows indicate the elution volume for calibration proteins thyroglobulin (A = 670 kD), apoferritin (B = 443 kD), alcohol dehydrogenase (ADH) (C = 150 kD), and NaCl (D). The peaks on the curve from the right represent NaCl (1); monomers (2); and tetramers, hexamers and larger complexes (3–5).

### Gel Permeation Chromatography

Gel permeation chromatography was used to determine the molecular weights of complexes formed between TS1 and  $\alpha$ TS1. This was done using a Superose 6 column (Pharmacia), with a recommended separation range between 5 and  $5 \times 10^3$  kD, and a fast protein liquid chromatography (FPLC) system. The column was calibrated using gel filtration molecular weight markers GF-3 (Sigma, Stockholm, Sweden) (Fig. 1). The Abs, purified using protein G columns (Amersham Biosciences, Uppsala, Sweden), were dialyzed against phosphate-buffered saline pH 7.4 (8.1 mM Na<sub>2</sub>HPO<sub>4</sub>, 1.8 mM KH<sub>2</sub>PO<sub>4</sub>, 138 mM NaCl, 2.7 mM KCl) and subsequently mixed at 1:0.5, 1:1, and 1:2 ratios. The incubation time was 30 minutes and the chromatography was performed using a flow rate of 0.5 mL/min. As a control, polyclonal, affinity-purified rabbit antimouse IgG (Dakopatts AB, Älvsjö, Sweden) was mixed with MAb in the same ratios and analyzed similarly. The chromatograms were evaluated using PeakAlyze (Biosoft, Cambridge, United Kingdom).

### Gel Electrophoresis

Nondenaturing native polyacrylamide gel electrophoresis (PAGE) was performed on a Native PAGE PhastGel gradient 4–15%, with a separation range between 70 and 700 kD, using a PhastSystem (Pharmacia). The electrophoresis was run for 600 Vh and stained with Coomassie brilliant blue. For molecular

weight determination, a high-molecular-weight kit marker was used (Pharmacia). The Abs were mixed 1:0.5, 1:1, and 1:2 and incubated for 30 minutes before being subjected to electrophoresis. As a control, polyclonal, affinity-purified rabbit antimouse IgG (Dako) was mixed with MAb in the same ratios and run on the gel.

### Electron Microscopy

Analyses of MABs and immune complexes were performed by negative stain transmission electron microscopy as previously described.<sup>16,17</sup> Whole molecule reactants were mixed at a 1:1 molar ratio in buffered saline borate (BSB, 100 mM H<sub>3</sub>BO<sub>3</sub>, 25 mM Na<sub>2</sub>B<sub>4</sub>O<sub>7</sub>, 75 mM NaCl, pH 8.2) at 2 mg/mL (1 mg/mL of each MAb), 0.2 mg/mL, and 0.02 mg/mL and incubated at room temperature for 20 minutes. Following incubation, the reactants were affixed to carbon membranes, stained with uranyl formate, and mounted on copper grids for analysis. Just before sampling, the 2-mg/mL and 0.2-mg/mL samples were diluted to 0.02 mg/mL with BSB to prevent the attachment of excess protein to the mounting membrane. Electron micrographs were recorded at  $\times 50,000$  or  $\times 100,000$  magnification on a JEOL CX 1200 transmission electron microscope. Scoring of immune complexes as rings or chains was performed directly on the electron micrographs with the aid of a hand-held lens. Estimates were made of the number of Abs in some of the larger complexes, since these tended to fold back on themselves, obscuring some of the detail needed to make precise subunit counts. At least 1300 molecules were scored for each sample. All scoring was performed blind.

### Radiolabeling

The MABs were radiolabeled with <sup>125</sup>I (IMS 30, Amersham) using the chloramine T method. Free iodine was removed by passage over a Sephadex G 50 column (Pharmacia).

### In Vivo Clearing of Radiolabeled Idiotype Using Anti-Idiotype

Eighteen female nude mice (Balb/c nu/nu, Bomholtgaard, Denmark) were divided into Groups A–D, where Group A served as the control receiving the radiolabeled Id only. All mice received an intraperitoneal injection of 48  $\mu$ g of the <sup>125</sup>I-labeled Id MAb, TS1. Twenty-four hours later, the mice in Group B were injected intraperitoneally with 12  $\mu$ g of the unlabeled anti-Id MAb  $\alpha$ TS1, i.e., a TS1: $\alpha$ TS1 ratio of 1:0.3 (after taking into consideration the biologic turnover of the Id during the first 24 hours). Mice in Group C were injected with 24  $\mu$ g of  $\alpha$ TS1, a 1:0.6 ratio. Finally, Group D mice received 48  $\mu$ g of  $\alpha$ TS1, which represents a 1:1.2 ratio.

The total-body activity of each mouse was measured at 1, 4, 7, 10, and 13 hours postinjection, using a Maxi Camera II (General Electric, West Milwaukee, WI), connected to a Hermes evaluation unit (Hermes ver. 2.3B, Nuclear Diagnostics, Hägersten, Sweden). To avoid anesthesia, the mice were kept in a small box during measurements, at a constantly fixed distance from the camera.

### Measurements of Activity Uptake in Different Organs during Anti-Idiotype-Mediated Idiotype Clearance

Twenty-one female nude mice (Balb/c nu/nu, Bomholtgaard, Denmark) were divided into five groups, A–E. Each mouse was injected intraperitoneally with 50  $\mu$ g of the Id MAb TS1. After 24 hours, each mouse received a 10- $\mu$ g intravenous injection of the <sup>125</sup>I-labeled anti-Id MAb  $\alpha$ TS1, with a specific activity of 192 MBq/mg. The five groups of animals were sacrificed after 1, 4, 7, 10, and 13 hours after anti-Id injection. Blood samples and internal organs were harvested and weighed, and their activity was measured using a gamma counter (1282 Compugamma, Uppslands Väsby, Sweden). In addition, a control experiment was performed in a similar fashion in which the mice received only the <sup>125</sup>I-labeled anti-Id.

## RESULTS

### Gel Permeation Chromatography

As illustrated in Figure 1, the shape of the elution profile indicates considerable size heterogeneity with at least three predominant peaks. All complexes, formed in vitro, were larger than  $1 \times 10^3$  kD when TS1: $\alpha$ TS1 were mixed in 1:0.5, 1:1, and 1:2 molar ratios. The 1:1 mixture (shown in the figure) displayed peaks representing three different complex formations with apparent molecular weights of  $1.1 \times 10^3$ ,  $3.0 \times 10^3$ , and  $4.0 \times 10^3$  kD, representing approximately 75% of the MAb protein content (Fig. 1, peaks 3, 4, and 5, respectively). MAb mixtures of 1:0.5 and 1:2 ratios showed peaks at  $1.1 \times 10^3$  and  $1.7 \times 10^3$  kD. Control mixture of the affinity-purified rabbit antimouse Ig and MAb at a 1:1 ratio showed a broad peak between 370 and  $3.1 \times 10^3$  kD with a maximum height at 690–700 kD. Furthermore, a peak at 280 kD could be seen. In control mixtures at the ratios 1:0.5 and 1:2, the 280-kD peak increased in area. All Abs, when analyzed alone, had molecular weights between 145 and 170 kD.

### Gel Electrophoresis

The native PAGE, performed on Native PAGE PhastGel gradient (4–15%), illustrated a protein pattern in which more than 70% of the material was found in complexes corresponding to molecular weights larger than 670 kD (Fig. 2), as determined using Quantiscan

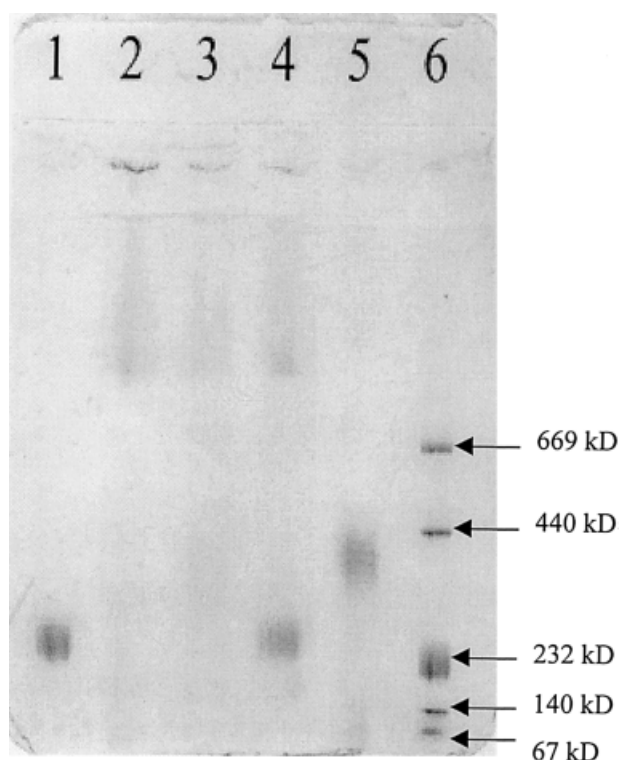


**FIGURE 2.** Native polyacrylamide gel electrophoresis gradient 4–15% gel. Lane 1, TS1; Lane 2, equimolar mixtures of TS1 and  $\alpha$ TS1; Lane 3, TS1: $\alpha$ TS1 at a 1:0.5 ratio; Lane 4, TS1: $\alpha$ TS1 at a 1:2 ratio; Lane 5,  $\alpha$ TS1; Lane 6, MW marker showing bands of the sizes 669 kD, 440 kD, 232 kD, 140 kD, and 67 kD. Using Quantiscan, it was determined that more than 70% of the MAbs had formed complexes larger than 669 kD.

(BioPlot). No direct correlation between molecular weight and mobility can be expected in native gels. The polyclonal rabbit anti-mouse IgG and mAb mixtures partially remained at the application site (data not shown).

#### Electron Microscopy of Idiotypic and Anti-Idiotypic Interaction Patterns

To directly count the number of Ig molecules in the individual Id–anti-Id complexes and to assess the effect of concentration on immune complex formation, equimolar concentrations of Id and anti-Id MAb were mixed at three different concentrations (2.0, 0.2, and 0.02 mg/mL, total protein) and incubated at room temperature for 20 minutes. Between 1,300 and 1,845 Ig molecules were scored per sample. In each case, over 97% of the molecules were found to be in complex, attesting to the near-equal molar ratio and the high affinity of the reactants. One of the most striking observations was that essentially none of the complexes appeared as ring dimers, the predicted geometry of Id–anti-Id complexes in the absence of steric

constraints. As seen in Table 1, the largest class of complexes was ring tetramers followed by ring hexamers and ring octamers. Larger rings with up to 16–20 members were also observed. The linear (chain) complexes included mostly trimers followed by progressively fewer numbers of pentamers and heptamers and larger-sized complexes. Very few open chain dimers were observed. Of the scorable examples, ring forms outnumbered chain forms by more than 2:1. A comparison of the results of incubation at different concentrations showed that the higher concentration of Id and anti-Id (2mg/mL) with a molar ratio of 1:1 favors the formation of larger complexes. This could be seen by comparing the percentages of molecules forming tetrameric rings (26.8% at 2 mg/mL vs. 39% at 0.02 mg/mL) and those forming complexes having greater than eight members (31.4% at 2 mg/mL vs. 11.5% at 0.02 mg/mL) (Table 1). An illustration of the electron microscopy results is displayed in Figure 3.

#### In Vivo Clearing of Radiolabeled Idiotype Using Anti-Idiotypic

In the control group, Group A, which received the radiolabeled Id only, there was a 40% excretion of radioactivity from the mice over the study period (70 hours), as seen in Figure 4A. The controls showed a stable decline in activity over time (half-life approximately 4 days), whereas the other groups displayed a significant reduction of activity over the first 20 hours after anti-Id injection. The activity decrease for Group A, from 24 hours to 70 hours, was 25%. The corresponding decrease for Group B after anti-Id injection (TS1: $\alpha$ TS1 1:0.3) was 40%, for Group C (1:0.6) 54%, and for Group D (1:1.2) 85%. Twenty-four hours after injection of  $\alpha$ TS1, the rate of activity decrease in all experimental groups was similar to that of the controls, indicating that the anti-Id had exerted its effect during the first 24 hours after injection.

#### Measurements of Activity Uptake in Different Organs during Clearance of the Idiotype Using the Anti-Idiotypic

The activity uptake in different organs during clearance of the Id using the anti-Id can be seen in Figure 4B and C, and illustrates the amount of activity in different tissues at 1, 4, 7, 10, and 13 hours after anti-Id injection. One hour after injection of the radiolabeled anti-Id, a significant amount of radioactivity had been reallocated from the blood to the different organs in general, and to the liver in particular. The uptake of radiolabeled anti-Id in the liver is substantial, displaying a higher activity (displayed as cpm/g in Fig. 4B, and as relative activity per gram of tissue in Fig. 4C) than the blood and other organs 1 hour after radiolabeled anti-Id injection. After 4 hours, the activity values for liver and blood are more or less equal, as the

**TABLE 1**  
**Analysis of TS1- $\alpha$ TS1 Complexes by Electron Microscopy<sup>a</sup>**

Conc. (mg/mL)	1	2/-	3/-	4/0	5/-	6/0	7/-	8/0	>8/-	>8/0	>8/?	tot>8	Chain	Ring
2.0	4.8	0.8	4.8	26.8	5.3	11.9	2.7	6.1	10.6	14.4	6.4	31.4	27.2	66.6
0.2	7.4	0.4	7.6	40.5	4	10.7	3.4	6.5	8	10.3	0	18.3	25.3	73.4
0.02	6.6	1.2	11.5	39	6.9	10.7	4.3	6.6	4.3	6.6	0.6	11.5	30.3	67.8

<sup>a</sup>The top row indicates the complex type code: 1 = monomer, 2 = dimer, 3 = trimer, etc.; 4/0, 6/0, etc. indicate ring formation of 4 or 6 immunoglobulin (Ig)G molecules; 2/-, 3/-, 5/- etc. indicate chains of 2, 3, 5, etc. IgGs with no ringformation; >8/- indicates chains of >8 IgGs in length; >8/? indicates complexes of more than eight IgGs, which could not be clearly determined to be either a chain or a ring; tot >8 corresponds to the percentages of all complexes of >8. The results are displayed as % of molecules in the specified configuration. Chain and ring, respectively, correspond to the % of molecules in chains or rings after subtracting monomers and complexes that could not be categorized. The complex formation was studied at three different concentrations with equimolar amounts of both idiotypic and anti-idiotypic monoclonal antibody.

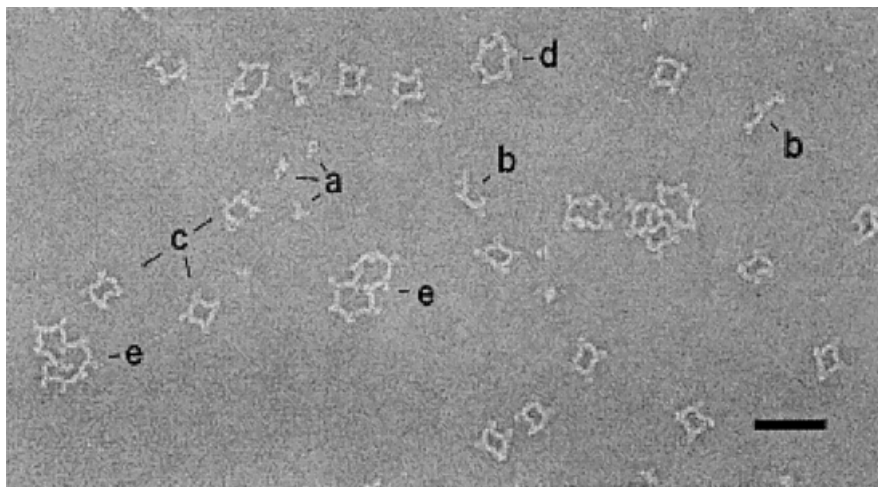


**FIGURE 3.** Electron micrograph of TS1 and  $\alpha$ TS1 immune complexes. The idiotypic and anti-idiotypic for this sample were mixed at 0.1 mg/mL each, incubated for 20 minutes, and diluted 10-fold just prior to mounting and staining. The electron micrograph shows unreacted molecules (a), chains of three (b), rings of four (c), a ring of six (d), and a ring of 10 (e).

activity in the liver begins to decrease and the blood activity increases. At 7 hours after anti-Id injection, the liver activity is steadily decreasing, while in the blood the activity has leveled off and is initiating a slight decrease. As seen in the controls in Fig. 4D, when the animals were injected with the <sup>125</sup>I-labeled anti-Id only, the liver uptake is similar to that of the other organs, indicating no specific uptake in this particular organ.

## DISCUSSION

The concept of using anti-Ids as clearing agents is not new,<sup>8,11,18</sup> but detailed information on the generation and catabolism of the formed immune complexes is limited. The current investigation proves, by use of PAGE, gel permeation chromatography, and electron microscopy, that the Id-anti-Id MAb pair TS1- $\alpha$ TS1 reacts to form a wide array of immune complex types. As indicated by PAGE and gel permeation chromatography, and confirmed by electron microscopy, 75–80% of the Ab material was found in the in vitro-generated complexes, which were predominantly ring structures composed of 4, 6, 8, or more immunoglob-

ulin molecules. Together, these rings of various sizes constituted more than 60% of the Id-anti-Id molecules in complex at equimolar mixture. These observations are in accordance with previous reports stating that equimolar mixtures of MAbs, for thermodynamic reasons, prefer to form ring-shaped complexes having the fewest possible components unless structurally constrained from doing so.<sup>19–23</sup> Interestingly, in the TS1- $\alpha$ TS1 system, dimers were rare, probably reflecting a location of epitopes incompatible with tight, dimeric interaction coupled with insufficient flexibility of the IgG<sub>1</sub> hinge regions to compensate for the resulting angular constraints, a phenomenon previously reported for other Id-anti-Id systems.<sup>10,20,24</sup> Previous electron microscopic studies have shown that idiotopes located at the very tip of the Fab arms are much less likely to form ring dimers than are those idiotopes whose orientations are slightly tangential to the long axis of the Fab.<sup>24,25</sup> Similar studies have also shown that the relative flexibility of the hinge region can dramatically influence immune complex morphology.<sup>19–21,26,27</sup> For example, for a matched set of Id-anti-Id reactions, differing hinges in the Id-

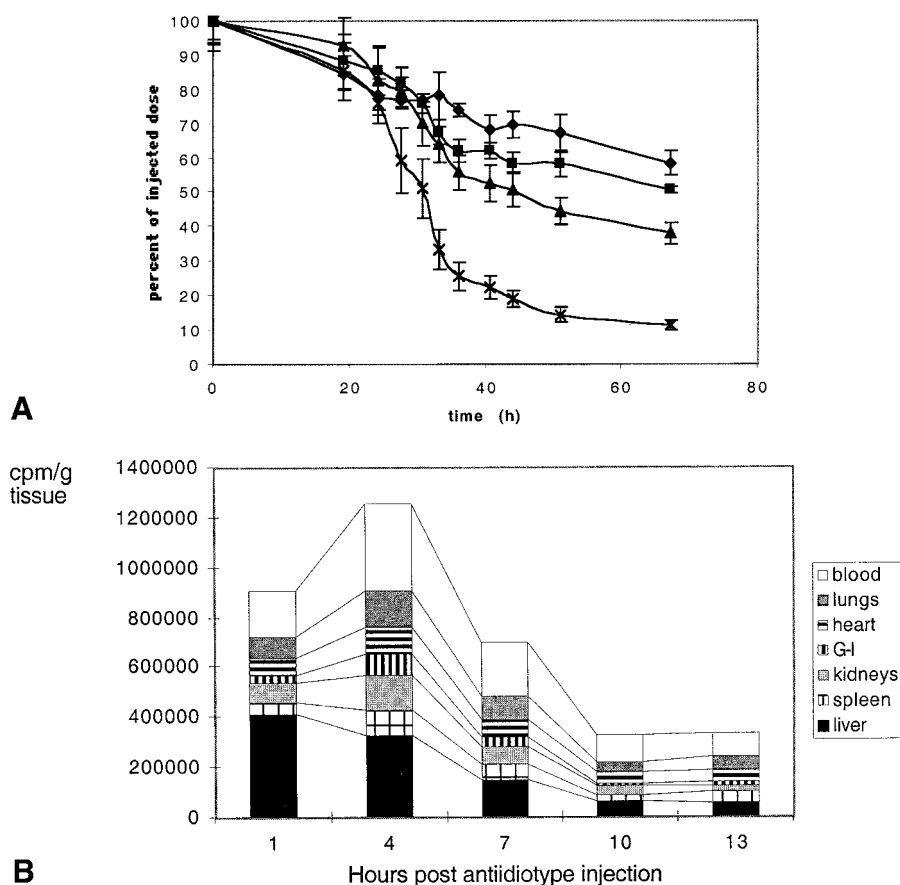
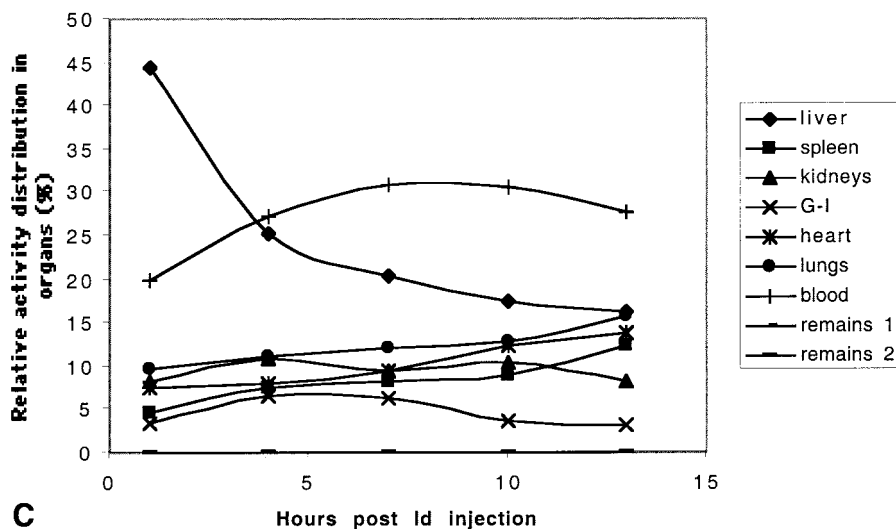


**FIGURE 4.** (A) Clearance of TS1 using  $\alpha$ TS1 in nude mice. All mice received an intraperitoneal injection of 48  $\mu$ g iodine-125 ( $^{125}$ I)-labeled TS1. Twenty-four hours later, Groups B–D were injected intraperitoneally with an amount of  $\alpha$ TS1 representing the following TS1: $\alpha$ TS1 ratios; diamonds represent Group A (controls receiving  $^{125}$ I-TS1 only), squares represent Group B (TS1: $\alpha$ TS1 ratio 1:0.3), triangles represent Group C (1:0.6), and X's represent Group D (1:1.2). Bars, standard deviation. (B) The activity uptake in different organs during clearance of TS1 using  $\alpha$ TS1 is shown (illustrated as cpm per gram of tissue) at 1, 4, 7, 10, and 13 hours after  $\alpha$ TS1 intravenous injection. After 1 hour, a substantial amount of radioactivity has been reallocated from the blood to the liver. After 4 hours, the activity in the liver has declined while the blood activity has increased. At 7 hours after  $\alpha$ TS1 injection, the liver activity has continued to decrease. (C) The relative activity distributions in different organs, expressed in %, during clearance of TS1 using  $\alpha$ TS1 is shown at 1, 4, 7, 10, and 13 hours after  $\alpha$ TS1 intravenous injection. After 1 hour, a substantial amount of radioactivity has been reallocated from the blood to the liver. After 4 hours, the activity in the liver has begun to decline while the blood activity is increasing. At 7 hours after  $\alpha$ TS1 injection, the liver activity is steadily decreasing while the blood activity levels off. (D) A control experiment shows the activity (cpm/g) in different organs after injection of  $^{125}$ I-labeled  $\alpha$ TS1 only.

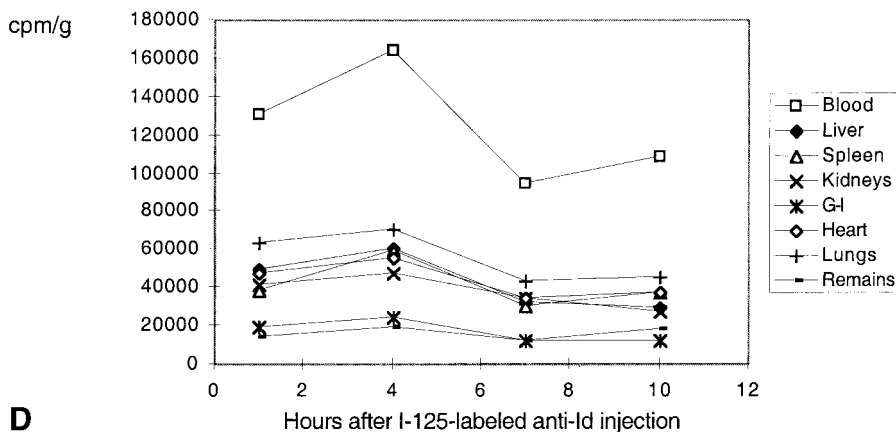
bearing molecule can lead to complexes devoid of ring dimers for one hinge type to complexes in which ring dimers almost exclusively predominate for another hinge type.<sup>19</sup> Ring dimers dominate when two fully flexible Abs interact, but any limitations of this flexibility, of steric hindrance, or of both, will force the equilibrium to shift toward rings composed of four or, if severely restricted, larger multiples of 2.<sup>19–23</sup> The concentration of the reactants also plays a role in the type of immune complexes generated. At low concentrations, where molecular interactions are less frequent, more time is allowed for each Id–anti-Id multiple of 2 to close the circle before binding to another molecule or complex, thus favoring smaller rings. The long-term fate of the variously sized complexes in vivo

will depend on the intricacies of the interplay between the relative affinity and structural characteristics of the reactants, differential compartmentalization, and the relative contribution of different clearance mechanisms.

The combined information from electron microscopy, gel permeation chromatography, and PAGE reveals the composition of these complexes more fully than any of the individual techniques alone. It appears reasonable that the apparent molecular weights of the complexes tend to be overestimated by techniques that are based on mobility or movement, since such techniques separate proteins based on Stokes radius or size, and the unique open-ring geometry of each complex leaves significant space between the individ-



C



D

FIGURE 4. (continued)

ual Ab molecules, as visualized by the electron microscopy studies. This open and variable conformation makes Id-anti-Id complexes, as proteins, rather atypical from a mobility point of view.

This in vivo investigation demonstrates that it is possible to selectively reduce the levels of an administered MAb by use of its cognate anti-Id in a stoichiometric way. More than 80% of redundant radiolabeled MAb remaining in the circulation can be complexed, degraded, and subsequently excreted via the urine within 24 hours, thus providing a means of significantly decreasing the undesirable side effects caused by circulating, nontargeted radiolabeled MAbs. The finding that large complexes predominate in this system, as compared with smaller dimeric rings in other systems, may influence the clearance rate of the complexes. Formation of large complexes both inside and outside the vasculature might, in fact, facilitate their rapid and efficient uptake and degradation. Attempts to isolate such complexes from blood in vivo

have not yet been successful, possibly due to the rapid removal from the circulation (unpublished data).

The metabolism of the immune complexes between Id and anti-Id occurs mainly in the liver.<sup>28,29</sup> As can be seen in Figure 4B and C, substantial levels of anti-Id have accumulated in the liver by 1 hour after anti-Id injection. A similar time interval for liver accumulation has previously been reported for immune complexes formed between antigens and Abs.<sup>29</sup> By 4 hours, degradation has certainly commenced, as illustrated by the increase in blood activity. The passage of nuclide through the liver, and subsequent secretion of iodine through the kidneys, is transient and relatively rapid and should therefore not cause significant radiotoxic damage to these organs. Previous studies have suggested that some immune complex degradation also occurs in the spleen; however, this was been verified in the current study. The mechanisms responsible for the elimination of complexes are open to speculation. It is known that both Kupffer cells and

sinusoidal endothelial cells in the liver express Fc receptors and are involved in the clearance of immune complexes from the circulation.

The relative ratio between nonspecific phagocytic uptake and Fc receptor–mediated uptake remains to be further studied. However, it has been reported that at low anti-Id:Id ratios the relative uptake in the spleen is higher than at higher ratios, indicating that size or molecular composition of the complexes may play a role in regulating the route of the complex metabolism.<sup>30</sup> Since Fc receptors are widely distributed throughout the body, yet the largest relative uptake takes place in the liver, there may be alternative pathways for uptake and degradation of complexes in this particular organ.

## REFERENCES

- De Nardo GL, O'Donnell RT, Kroger LA, Richman CM, Goldstein DS, Shen S, et al. Strategies for developing effective radioimmunotherapy for solid tumors. *Clin Cancer Res* 1999; 5(Suppl):3219s–3223s.
- De Nardo SJ, Kroger LA, De Nardo GL. A new era for radio-labeled antibodies in cancer. *Curr Opin Immunol* 1999;11: 563–9.
- Potamianos S, Varvarigou AD, and Archimandritis SC. Radioimmunoscintigraphy and radioimmunotherapy in cancer: Principles and application. *Anticancer Res* 2000;20:925–48.
- Pedley R, Boden J, Boden R, Dale R, Begent R. Comparative radioimmunotherapy using intact or F(ab')<sub>2</sub> fragments of 131I anti-CEA antibody in a colonic xenograft model. *Br J Cancer* 1993;68:69–73.
- Yokota T, Milenic DE, Whitlow M, Schlom J. Rapid tumor penetration of a single-chain Fv and comparison with other immunoglobulin forms. *Cancer Res* 1992;52:3402–8.
- Begent RH, Verhaar MJ, Chester KA, Casey JL, Green AJ, Napier MP, et al. Clinical evidence of efficient tumor targeting based on single-chain Fv antibody selected from a combinatorial library. *Nat Med* 1996;2:979–84.
- Garkavij M, Tennvall J, Strand SE, Nilsson R, Lindgren L, Chen J, et al. Extracorporeal immunoadsorption from whole blood based on the avidin-biotin concept: evaluation of a new method. *Acta Oncol* 1996;35:309–12.
- Begent RH, Bagshawe DK, Pedley RB, Searle F, Ledermann JA, Green AJ, et al. Use of second antibody in radioimmunotherapy. *Natl Cancer Inst Monogr* 1987;3:59–61.
- Ullén A, Sandström P, Riklund Åhlström K, Sundström B, Nilsson B, Årlestig L and Stigbrand T. Use of anticytokeratin monoclonal anti-idiotypic antibodies to improve tumor: nontumor ratio in experimental radioimmunotargeting. *Cancer Res* 1995;55(Suppl):5868s–5873s.
- Casey JL, King DJ, Pedley RB, Boden JA, Boden R, Chaplin LC, et al. Clearance of yttrium-90–labelled anti-tumor antibodies with antibodies raised against the 12N4 DOTA macrocycle. *Br J Cancer* 1998;78:1307–12.
- Ullén A, Riklund Åhlström K, Hietala S-O, Nilsson B, Årlestig L, Stigbrand T. Secondary antibodies as tools to improve tumor to nontumor ratio at radioimmunolocalisation and radioimmunotherapy. *Acta Oncol* 1996;35:281–5.
- Johansson A, Sandström P, Ullén A, Behravan G, Erlandsson A, Levi M, et al. Epitope specificity of the monoclonal anticytokeratin antibody TS1. *Cancer Res* 1999;59:48–51.
- Riklund Åhlström K, Ullén A, Makiya R, Sundström B, Thornell L-E, Stigbrand T. Radioimmunotherapy of HeLa cell tumors in nude mice by a combination of iodine-131–labelled monoclonal antibodies against placental alkaline phosphatase and cytokeratin. *Tumor Targeting* 1995;1:239–44.
- Ullén A, Sandström P, Rossi Norrlund R, Rathsmann S, Johansson L, Riklund Åhlström K, et al. Dosimetry of fractionated administration of <sup>125</sup>I–labeled antibody at experimental radioimmunotargeting. *Cancer* 1997;80(Suppl):2510–2518.
- Sundström B, Nathrath WBJ, Stigbrand T. Diversity in immunoreactivity of tumor-derived cytokeratin monoclonal antibodies. *J Histochem Cytochem* 1989;37:1845–54.
- Roux KH. Immunoelectron microscopy of idiotype–anti-idiotype complexes. *Methods Enzymol* 1989;178:130–44.
- Roux KH. Negative-stain immunoelectron-microscopic analysis of small macromolecules of immunologic significance. *Methods* 1996;10:247–56.
- Sharkey R, Primus J, Goldenberg D. Second antibody clearance of radiolabeled antibody in cancer radioimmunodetection. *Proc Natl Acad Sci U S A* 1984;81:2843–6.
- Roux KH, Strelets L, Brekke OH, Sandlie I, Michaelsen TE. Comparisons of the ability of human IgG3 hinge mutants, IgM, IgE and IgA2 to form small immune complexes: a role for flexibility and geometry. *J Immunol* 1998;161:4083–90.
- Roux KH, Strelets L, Michaelsen TE. Flexibility of human IgG subclasses. *J Immunol* 1997;159:3372–82.
- Schumaker VN, Phillips ML, Hanson DC. Dynamic aspects of antibody structure. *Mol Immunol* 1991;28:1347–60.
- Murphy RM, Chamberlin RA, Schurtenberger P, Colton CK, Yarmush ML. Size and structure of antigen-antibody complexes: thermodynamic parameters. *Biochemistry* 1990;29: 10889–99.
- Dangl JL, Wensel TG, Morrison SL, Stryer L, Herzenberg LA, Oi VT. Segmental flexibility and complement fixation of genetically engineered chimeric human, rabbit and mouse antibodies. *EMBO J* 1988;7:1989–94.
- Phillips ML, Oi VT, Schumaker VN. Electron microscopic study of ring-shaped, bivalent hapten, bivalent antidansyl monoclonal antibody complexes with identical variable domains but IgG1, IgG2a and IgG2b constant domains. *Mol Immunol* 1990;27:181–90.
- Roux KH, Greenspan NS. Monitoring the formation of soluble immune complexes composed of idiotype and anti-idiotype antibodies by electron microscopy. *Mol Immunol* 1994;31:599–606.
- Moyle WR, Lin C, Corson RL, Ehrlich PH. Quantitative explanation for increased affinity shown by mixtures of monoclonal antibodies: importance of a circular complex. *Mol Immunol* 1983;20:439–52.
- Chan LM, Cathou RE. The role of the inter-heavy chain disulfide bond in modulating the flexibility of the immunoglobulin G antibody. *J Mol Biol* 1977;112:653–6.
- Skogh T, Blomhoff R, Eskild W, Berg T. Hepatic uptake of circulating IgG immune complexes. *Immunology* 1985;55: 585.
- Kosugi I, Muro H, Shirasawa H, Ito I. Endocytosis of soluble IgG immune complex and its transport to lysosomes in hepatic sinusoidal endothelial cells. *J Hepatol* 1992;16:106–14.
- Sharkey RM, Blumenthal RD, Goldenberg DM. Anti-antibody enhancement of tumor imaging. *Cancer Treat Res* 1990;51:433–55.